

Synthesis and Characterization of Polyaniline -Crooked Gold Nanocomposite with Reduced Conductivity

R. Hawaldar^{1,2}, M. Kulkarni¹, S. Jadkar², U. Pal³
and D. Amalnerkar^{1, a}

¹International Institute of Information Technology, P-14, Pune Infotech Park, Hinjawadi, Pune 411 057, India.

²Department of Physics, University of Pune, Pune-411007, India.

³Instituto de Física, Universidad Autónoma de Puebla, Puebla, Pue. 72570, Mexico.

^adpa54@yahoo.com (corresponding author)

[Received: August 3rd, 2007; revised: January 16th, 2008; Accepted: January 23rd, 2008]

Keywords: Conducting Polymer, Polyaniline, Gold-Nanocomposite, Spectroscopy, Morphology.

Abstract. Conducting Polyaniline (Pani)-crooked Gold nanocomposites were synthesized by *in situ* chemo-oxidative polymerization of aniline with previously made crooked gold nanoparticles by using ammonium per oxidisulphate as oxidizing agent and p-toluene sulphonic acid (p-TSA) as dopant. The formation of nano gold was established by UV-visible spectroscopy with a SPR peak at 512 nm and crooked morphology was confirmed by TEM. Spectroscopic analysis confirmed the formation of the conducting emeraldine salt phase of the polymer. Due to clustering of composite nanoparticles, the polymer composite formed one-dimensional rod-like morphologies. Thermogravimetric analysis revealed a typical three-step decomposition pattern pertaining to polyaniline emeraldine salt. The conductivity of the nanocomposite was found to be lower (2.47 S/cm) than the virgin p-TSA doped polyaniline (5.55 S/cm).

Introduction

Inherently conducting polymers (ICPs) and other organic materials are uniquely suited for thin film, large area, mechanically flexible, low cost electronic devices [1,2]. Their tremendous commercial potential has touched off a flurry of research, particularly on organic light-emitting diodes [3,4], transistors [5,6], solar cells [7,8], memory devices [9-14] and sensors [15-18]. Among the conducting polymers, polyaniline (Pani) has received a great deal of attention owing to its simple synthesis, good environmental stability, ability to dope with protonic acids and moderately high electrical conductivity and is found to be a promising candidate for technological applications [3-8,15-18a]. The synthesis and characterization of Pani using a variety of synthetic methods and analysis techniques is well documented [17]. Of late, Pani/metal composite properties have been investigated [18b,18c] owing to novel electrocatalytic and sensing applications of Pani/Pt [19] and Pani/Pd [20]. In many cases, the incorporation of metal clusters in the polymer matrix also provides discrete reaction sites that can be probed electrochemically. Therefore, a conducting polymer decorated with metallic or semiconducting nanoparticles provides an exciting system to investigate with the possibility of designing device functionality [21a,21b]. It has also been reported that by using nanoscale materials, fabrication of high-density electronic devices are possible with superior performance and manufacturability [21,22].

The aim of the present work is to synthesize the polyaniline-gold nanocomposite by using p-TSA as dopant and to obtain the structural information by studying its physico-chemical properties using various analytical techniques such as UV-Visible spectroscopy, Fourier-transform infra-red

(FT-IR) spectroscopy, scanning electron microscopy (SEM), thermogravimetric analysis (TGA), and conductivity measurements.

Experimental

A) Preparation of gold nanoparticles

Crooked gold nanoparticles were prepared by surfactant-free reduction method [23]. Sodium borohydride was used to reduce aqueous 10^{-4} M solution of HAuCl_4 at room temperature (RT), in absence of any surfactant. The as synthesized products were characterized by UV-vis spectroscopy and transmission electron microscopy (TEM).

B) Preparation of Polyaniline-gold nanocomposite

All the chemicals and monomer used were of AR grade and used as received. The solutions were prepared using doubly distilled water. The polymerization was initiated by the drop wise addition of the oxidizing agent, 0.5M $(\text{NH}_4)_2\text{S}_2\text{O}_8$ (dissolved in minimum amount of water) in an acidified solution of 0.5M aniline containing crooked gold nanoparticles under constant stirring at 0-5 °C. The monomer to oxidizing agent ratio was kept as 1:1. Insitu doping was carried out by adding 1 Mole of para-toulene sulfonic acid (p-TSA) to make the composite conducting. After complete addition of the oxidizing agent, the reaction mixture was kept under stirring for 24 hours. The greenish black precipitate of the polymer was isolated by filtration and conditioned by washing and drying at 60 °C in an oven. UV-Vis spectra of the polymer solutions in m-cresol were recorded by using Hitachi-U3210 spectrophotometer in the range of 300-900 nm. Fourier transform infra-red (FT-IR) spectra of the polymers were recorded on a Perkin-Elmer-Spectrum 2000 spectrophotometer in the 400-4000 cm^{-1} spectral range. For FT-IR study, the samples were prepared in the pellet form using dry spectroscopic grade KBr powder. X-ray diffractograms (XRD) of the samples were recorded on a Rigaku (Miniflex Model, Japan) x-ray Diffractometer. Morphological studies were performed with the help of a Philips XL-30 Scanning Electron Microscope. Thermograms of the polymer samples were recorded using a Mettler-Toledo 851 thermogravimetric analyzer in N_2 atmosphere from RT to 900 °C with a heating rate of 10 °C/ min. The room temperature electrical conductivity of the samples was measured by two-probe measurement technique.

Results and Discussion

To determine the morphology of the as prepared gold nanoparticles, transmission electron microscopy studies were preformed. Formation of crooked gold nanoparticles can be clearly evinced from their TEM images (Fig. 1). Furthermore, to confirm the formation of gold nanostructures, the optical absorption spectra of the samples were recorded in the 200-800 nm spectral range. The optical absorption spectrum of the as prepared gold sample displays a SPR peak at 516 nm, with additional peaks at 377 nm, 260 nm and 211 nm, respectively (Fig. 2a). The origin of these additional peaks is unknown at this stage and further study towards their assignment is underway.

UV-visible spectroscopy is a very sensitive tool for the studies of protonation as well as for the elucidation of the interactions between the solvent, the dopant and the polymer chains. Fig. 2(b) shows the optical absorption spectrum of the polyaniline-gold nanocomposite doped with p-TSA, recorded by using m-cresol as a solvent. In m-cresol, polyaniline-gold nanocomposite exhibits three peaks at 320 nm, 420 nm and increasing absorption ~ 820 nm. The peak at 320 nm is sharp and corresponds to the π - π^* transition of the benzenoid rings, while a sharp and intense peak at 420 nm

can be attributed to the localized polarons which are the characteristics of the protonated polyaniline. The rise in absorption around 820 nm is owing to free carrier tail, characteristic of extended coil conformation of the conducting emeraldine salt phase of the polymer [24]. The spectral features observed in Fig. 2(b) reveals the enhanced solubility of polymer nanocomposite doped with p-TSA in m-cresol. On careful examination of the spectrum, it is noticed that the small hump ~ 660 nm for the p-TSA doped polymer nanocomposite is the representative of the insulating pernigraniline phase of the polyaniline. The extended tail at higher wavelength depicts that m-cresol not only serves as a solvent but also acts as an “efficient secondary dopant” [25]. MacDiarmid and Epstein introduced the term “efficient secondary doping” to describe the interaction of m-cresol and other phenols with protonated polyaniline. The m-cresol interacts more strongly with the polymer chain and/or with the dopant ion, consistent with a progressive change in molecular conformation from ‘compact coil’ to ‘extended coil’.

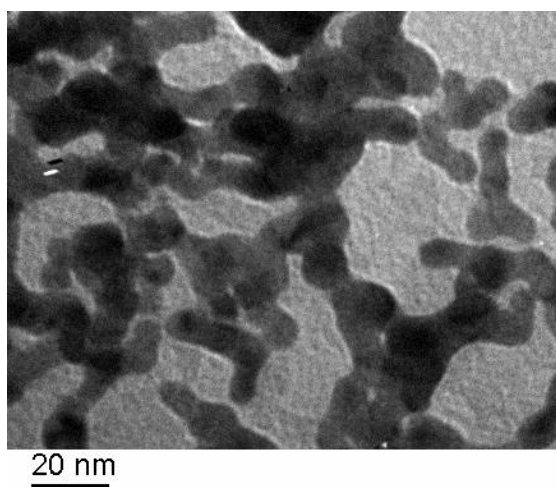


Figure 1. TEM image of crooked gold nanostructures.

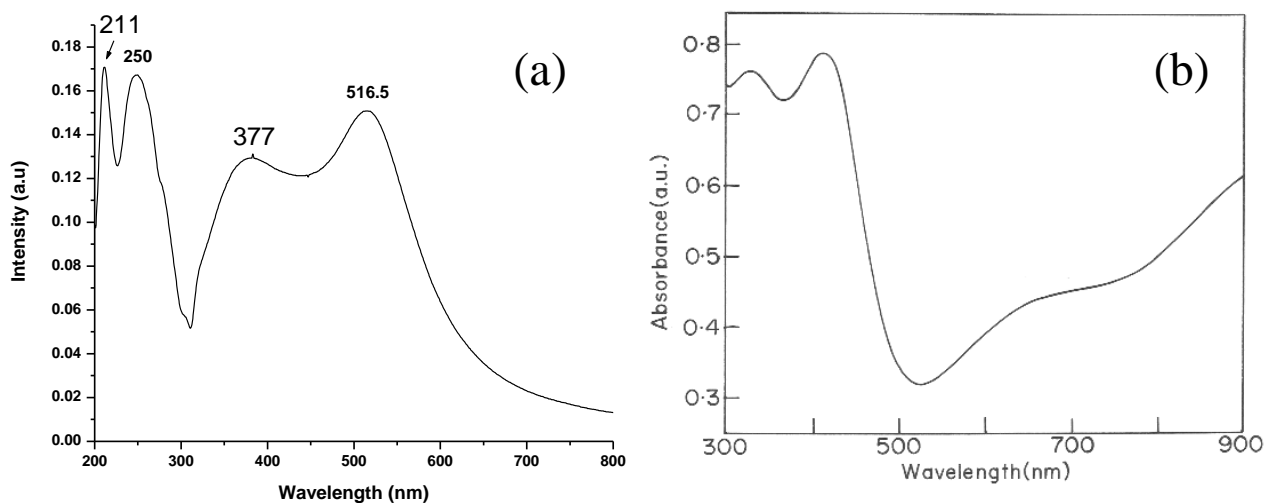


Figure 2. (a) UV-Visible Spectrum of Crooked -Gold nanostructures and (b) UV-Visible spectrum of Polyaniline-Gold nanocomposite

Fig. 3 represents the FT-IR spectrum of the polyaniline-gold nanocomposite doped with p-TSA, and the peak positions related to the corresponding chemical bonds are listed in Table 1. From the figure as well as from the Table 1, it is observed that the structure of the polymer nanocomposite is similar to that of the polyaniline, with characteristics modes of the polyaniline backbone with a very small variation. An intense band characteristic of para-di-substituted aromatic

rings through which polymerization proceeds is observed at $\sim 820 \text{ cm}^{-1}$. The strong band at $\sim 1125 \text{ cm}^{-1}$ is due to the vibration band of the dopant anion. Aromatic C-N stretching indicating secondary aromatic amine groups appears at $\sim 1300\text{-}1317 \text{ cm}^{-1}$. The presence of the two bands in the vicinity of 1500 cm^{-1} and 1600 cm^{-1} are assigned to the nonsymmetric C_6 ring stretching modes. The higher frequency vibration at 1600 cm^{-1} has a major contribution from the quinoid rings, while the lower frequency mode at 1500 cm^{-1} depicts the presence of benzenoid ring units. The presence of these two bands clearly indicates that the polymer is composed of the amine and imine units. Further, this also supports our UV-Vis absorption results, discussed earlier where, the different phases are observed in the spectrum. The presence of well-defined peak at $\sim 1032 \text{ cm}^{-1}$ related to the SO_3^- group shows the efficient incorporation of p-TSA into the polymer backbone.²⁴ The band at $\sim 3440 \text{ cm}^{-1}$ is assigned to the N-H stretching band. The presence of vibration bands of the dopant ion and other characteristic bands confirm the presence of conducting emeraldine salt phase in the polymer. Additionally, to ascertain the structural characteristic of the polyaniline-gold nanocomposite, X-ray diffraction studies of the samples were carried out. Fig. 4 shows a typical diffractogram of the nanocomposite confirming its amorphous nature. Only a broad peak related to polyaniline at $2\theta = 25^\circ$ can be seen in the XRD pattern. No peaks associated with gold were visible.

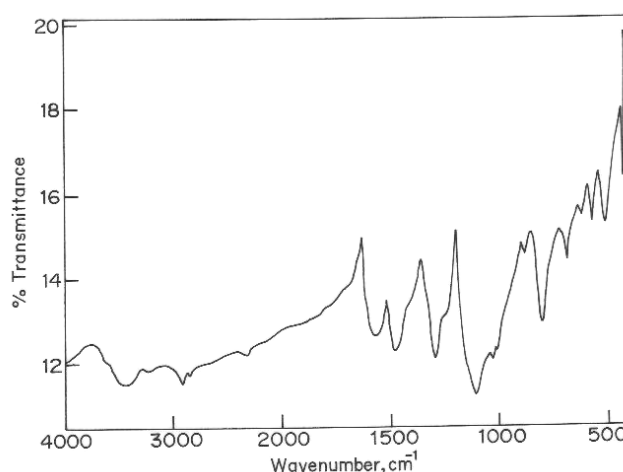


Figure 3. FT-IR Spectra of Polyaniline-Gold nanocomposite.

Table 1. Characteristic frequencies of chemically synthesized polyaniline –Gold nanoparticle composite.

Peak Position (Wave number cm^{-1})	Peak Assignment
676.49	C-H out of plane bending vibrations
794.47	Paradisubstituted aromatic rings indicating Polymer Formation
1107.83	C-H in plane bending vibration
1292.16	Aromatic C-N stretching indicating sec. aromating amine group
1476.49	C-N stretching due to benzenoid rings
1561.29	C-N stretching due to quinoid rings
2924.18	Aromatic C-H stretching vibration
3409.59	>N-H stretching vibrations

Fig. 5 shows the scanning electron micrographs of polymer nanocomposite. The magnifications were selected in such a way that the morphology could be observed clearly. The one dimensional rod-like morphology arising due to clustering of composite microparticles can be clearly seen in Fig. 5(a). The higher magnification images (Figs. 5 (b) and (c)) clearly evince the rod-like morphology. This could be quite natural since the gold nanoparticles were well dispersed in the reaction media with subsequent coating with the monomer. After addition of the oxidizing agent

under constant stirring, the polymerization preceded on these nuclei and grown as a rod like structure of the gold nanoparticles.

Figure 4. X-ray diffractogram of Polyaniline-Gold nanocomposite.

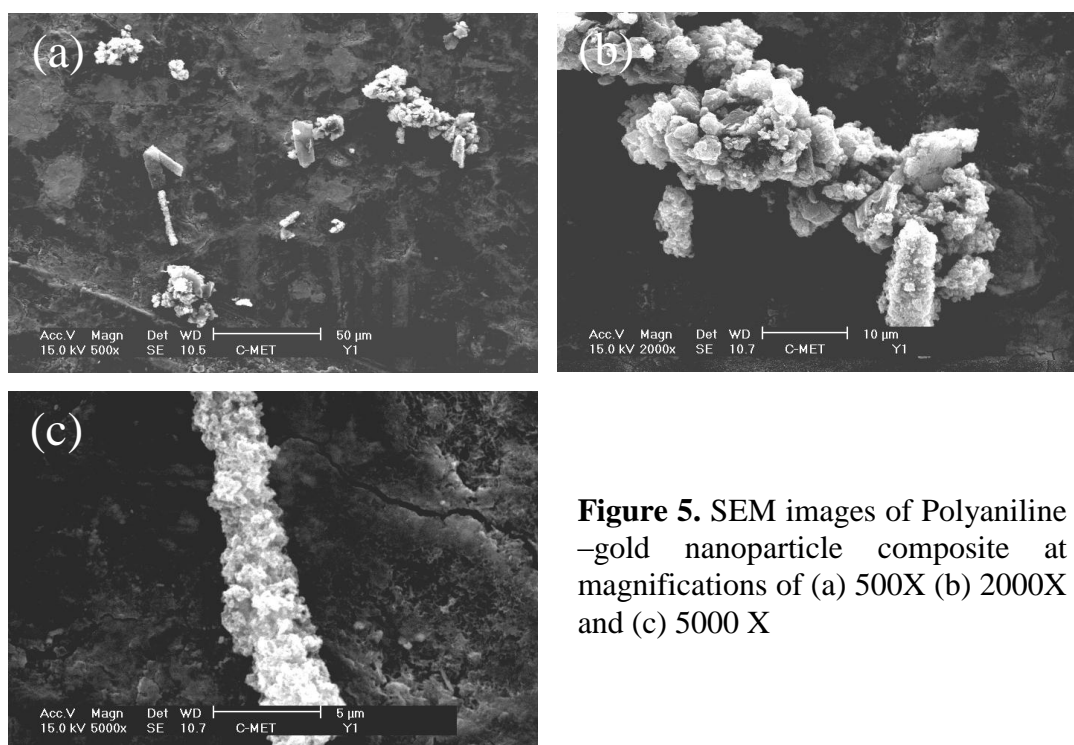
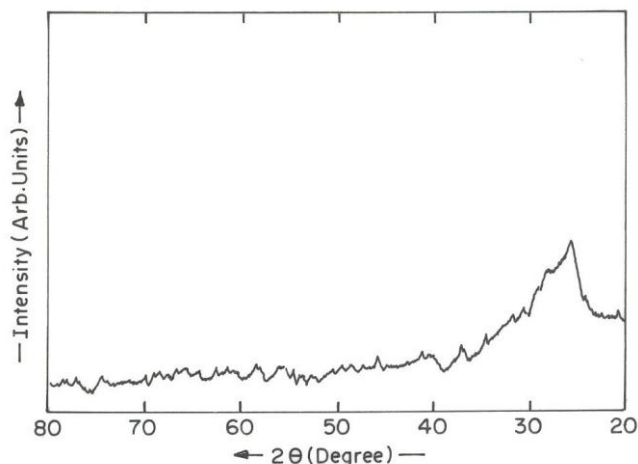


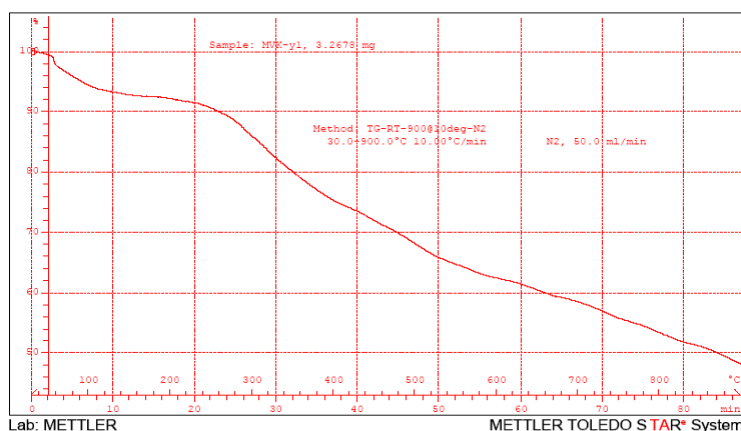
Figure 5. SEM images of Polyaniline –gold nanoparticle composite at magnifications of (a) 500X (b) 2000X and (c) 5000 X

Fig. 6 displays the thermal profile of the polymer nanocomposite. From the figure, it is observed that the polymer exhibits a three-step decomposition pattern similar to that of polyaniline. The first step in the decomposition pattern from room temperature to 100 °C is obviously due to the removal of free water molecules/moisture present in the polymer nanocomposite matrix. The second step loss starting from 120 to 300 °C is mainly because of the loss of the dopant ion from the polymer chains (thermal dedoping). Where as, the third step loss starting from 350 °C onwards is accounted for the degradation and decomposition of the skeletal polymer backbone after the elimination of the dopant ion [24].

The room temperature solid-state conductivity of the samples was measured on pressed pellets, having a diameter of 1.5 cm, using two-probe technique. The conductivity of the composite polyaniline sample (2.47 S/cm) is found to be lower than the virgin p-TSA doped polyaniline polyaniline, which was 5.55 S/cm. The exact origin of this anomalous reduction in conductivity is

unknown. However, such a reduction of conductivity in the composite sample can be attributed to the crooked gold nanoparticles in it, which are of very small in thickness, leading to a semiconductor like behavior.

Figure 6. Typical Thermogram of Polyaniline-Gold Nanocomposite.



Conclusions

Conducting Polyaniline (Pani) -Gold nanocomposite have been synthesized by in situ chemical oxidative polymerization method using ammonium per oxidisulphate as an oxidizing agent. p-Toulene sulphonic acid (p-TSA) was used as a dopant during the polymerization. The UV-Visible and FT-IR Spectroscopy confirmed the presence of conducting emeraldine salt phase of the polymer. Scanning electron microscopy (SEM) showed the rod like morphology of the polymer nanocomposite. Thermal studies revealed the typical three-step decomposition pattern pertaining to polyaniline emarldine salt. The anomalous lower conductivity of the nanocomposite might be attributed to the semiconducting behavior of the crooked gold nanostructures.

Acknowledgement

One of the authors R.Hawaladar is thankful to CNQS program of the Department of Physics, University of Pune for providing fellowship.

References

- [1] M.A. Baldo, D.F. O'Brien, Y. You, A. Shoustikov, S. Sibley, M.E. Thompson and S.R. Forrest, Nature Vol. 395 (1998), p. 151
- [2] F. Heringdorf, M.C. Reuter and R.M. Tromp, Nature Vol. 412 (2001), p. 517
- [3] R.H. Friend, R.W. Gymer, A.B. Holmes, J.H. Burroughes, R.N. Marks, C. Taliani, D.D.C. Bradley, D.A. Dos Santos, J.L. Brédas, M. Lögdlund and W.R. Salaneck, Nature Vol. 397 (1999), p. 121
- [4] C.D. Müller, A. Falcou, N. Reckefuss, M. Rojahn, V. Wiederhirn, P. Rudati, H. Frohne, O. Nuyken, H. Becher and K. Meerholz, Nature Vol. 421 (2003), p. 829
- [5] H. Siringhuas, N. Tessler and R.H. Friend, Science Vol. 280 (1998), p. 1741
- [6] C.D. Dimitrakopoulos and D.J. Mascaro, IBM J. Res. Dev. Vol. 45 (2001), p. 11
- [7] G. Yu, J. Gao, J.C. Hummelen, F. Wudl and A.J. Heeger, Science Vol. 270 (1995), p. 1789
- [8] C.J. Brabec, N.S. Sariciftci and J.C. Hummelen, Adv. Funct. Mater. Vol. 11 (2001), p. 15
- [9] J.C. Scott, Science Vol. 304 (2004), p. 62
- [10] Y. Chen, D.A.A. Ohlberg, X. Li, D.R. Stewart, R.S. Williams, J.O. Jeppesen, K.A. Nielsen, J.F. Stoddart, D.L. Olynick, and E. Anderson, Appl. Phys. Lett. Vol. 82 (2003), p. 1610

- [11] L.P. Ma, J. Liu and Y. Yang, *Appl. Phys. Lett.* Vol. 80 (2002), p. 2997
- [12] L.P. Ma, S. Pyo, J. Ouyang, Q.F. Xu and Y. Yang, *Appl. Phys. Lett.* Vol. 82 (2003), p. 1419
- [13] L.D. Bozano, B.W. Kean, V.R. Deline, J.R. Salem and J.C. Scott, *Appl. Phys. Lett.* Vol. 84 (2004), p. 607
- [14] J. Ouyang, C.W. Chu, C.R. Szmada, L.P. Ma and Y. Yang, *Nat. Mater.* Vol. 3 (2004), p. 918
- [15] A.A. Athawale and M.V. Kulkarni, *Sensors and Actuators B* Vol. 67 (2000), p. 173
- [16] M.V. Kulkarni and A.A. Athawale, *J. Appl. Polymer Sci.* Vol. 81 (2001), p. 1382
- [17] (a) M.V. Kulkarni and A.K. Viswanath, *Sensors and Actuators, B* Vol. 107 (2005), p. 791 (2005); (b) M.S. Cho, H.J. Choi, K.Y. Kim and W.S. Ahn, *Macromol. Rapid Commun.* Vol. 23 (2002), p. 713; (c) Y. Zhu, D. Hu, M. Wan, L. Jiang and Y. Wei., *Adv. Mater.* Vol. 19 (2007), p. 2092; (d) J. Han, G. Song and R. Guo, *Adv. Mater.* Vol. 00 (2000), p. 1; (e) H. Ding, M. Wan and Y. Wei, *Adv. Mater.* 19 (2007), p. 465
- [18] (a) M.V. Kulkarni, A.K. Viswanath and P.K. Khanna, *Sensors and Actuators, B* Vol. 115 (2006), p. 140; (b) J.M. Kinyanjui and D.W. Hatchett., *Chem. Mater.* Vol. 16 (2004), p. 3390; (c) S.K. Pillalamarri, F.D. Blum and M.F. Bertino, *Chem. Commun.* Vol. 36 (2005), p. 4584; (d) H. Cao, Z. Xu, H. Sang, D. Sheng and C. Tie, *Adv. Mater.* Vol. 13 (2001), p. 121
- [19] A.P. O'Mullane, S.E. Dale, T.M. Day, N.R. Wilson, J.V. Macpherson and P.R. Unwin, *J. Solid State Electrochem.* Vol. 10 (2006), p. 792
- [20] A. Mourato, S.M. Wong, H. Siegenthaler and L.M. Abrantes, *J. Solid State Electrochem.* Vol. 10 (2006), p. 140
- [21] (a) S. Tian, J. Liu, T. Zhu and W. Knoll, *Chem. Mater.* Vol. 16 (2004), p. 4103; (b) M. Riskin, B. Basnar, Y. Huang, and I. Willner, *Adv. Mater.* Vol. 19 (2007), p. 2691; (c) A.P. Alivisatos, *Science* Vol. 271 (1996), p. 933
- [22] J.W.G. Wildoer, L.C. Venema, A.G. Rinzler, R.E. Smalley and C. Dekker, *Nature* Vol. 391 (1998), p. 59
- [23] R. Hawaldar, R. Pasricha, U. Pal, S. Ogale and D. Amalnerkar (Unpublished results)
- [24] M.V. Kulkarni, A.K. Viswanath, R.C. Aiyer and P.K. Khanna, *J. Polymer Science: part B: Polymer Physics* Vol. 43 (2005), p. 2161
- [25] A.G. MacDiarmid and A.J. Epstein, *Synth. Met.* Vol. 65 (1994), p. 103

Journal of Nano Research Vol. 5

doi:10.4028/0-00000-029-9

Synthesis and Characterization of Polyaniline -Crooked Gold Nanocomposite with Reduced Conductivity

doi:10.4028/0-00000-029-9.79